Radiation induced defects in semiconductors: Optical study

Ivana Capan

Division of Materials Physics
Rudjer Boskovic Institute

http://www.irb.hr/users/capan

Outline

- Introduction
- Infrared spectroscopy (introduction and examples) →**IR**
- Photoluminescence (introduction and examples) → **PL**
- Conlusions

Introduction

- Besides electronically active defects, other centres give rise to a level falling in the valence or conduction band and are not active!!!
- However, such “neutral” radiation induced defects can affect the otical properties of the semiconductor, important for opto-electronic applications.
- Some of the deep-level defects also give rise to absorption bands.
- High density of defects for IR, may be far from the realistic operation condution.
- PL can be applied to low defect concentrations.

Infrared spectroscopy

- Infrared spectroscopy exploits the fact that molecules absorb specific frequencies that are characteristic of their structure. These absorptions are resonant frequencies, i.e. the frequency of the absorbed radiation matches the frequency of the bond or group that vibrates. IR radiation does not have enough energy to induce electronic transitions as seen with UV and visible light. Absorption of IR is restricted to excite vibrational and rotational states of a molecule.

- A molecule can vibrate in many ways, and each way is called a vibrational mode. For molecules with N atoms in them, linear molecules have 3N – 5 degrees of vibrational modes, whereas nonlinear molecules have 3N – 6 degrees of vibrational modes (also called vibrational degrees of freedom).

- Simple diatomic molecules have only one bond and only one vibrational band. If the molecule is symmetrical, e.g. N_2, the band is not observed in the IR spectrum, but only in the Raman spectrum. Asymmetrical diatomic molecules, e.g. CO, absorb in the IR spectrum. More complex molecules have many bonds, and their vibrational spectra are correspondingly more complex, i.e. big molecules have many peaks in their IR spectra.

Infrared spectroscopy

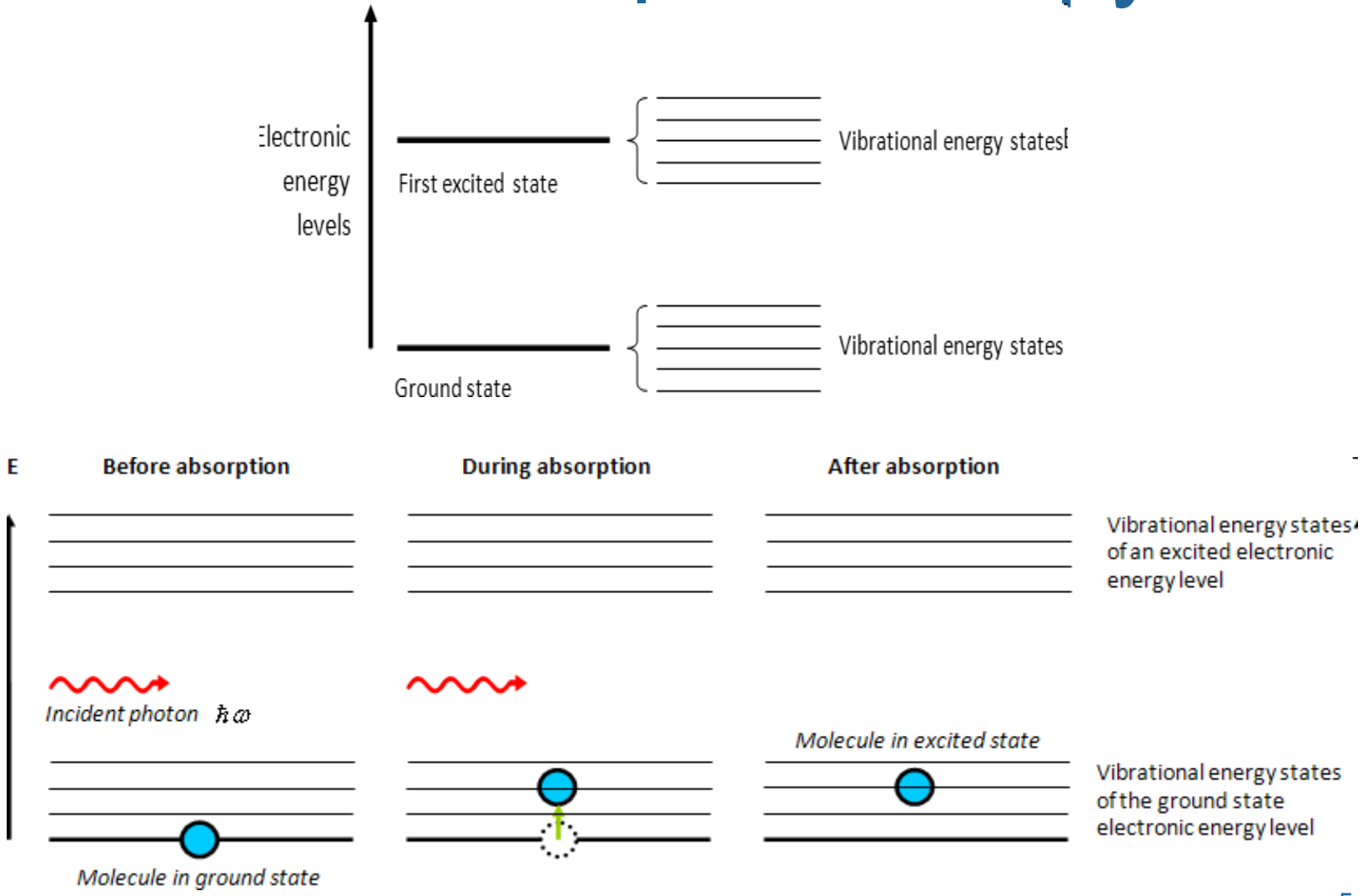

Infrared spectroscopy

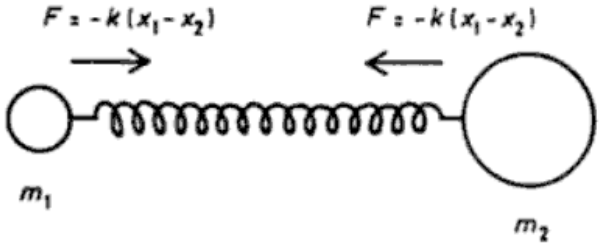

The vibration of a diatomic molecule with two atoms of mass m_1 and m_2. It happens that the frequency of vibration of molecules lies in the infrared region. Thus infrared radiation can be absorbed and transformed into molecular vibration.

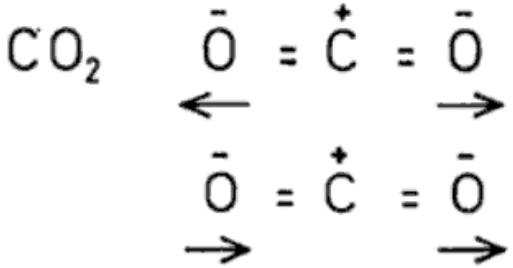

But... ←

Symmetric and asymmetric stretch modes of vibration for a carbon dioxide molecule. The symmetric stretch mode is not IR active but the asymmetric mode is IR active, whereas the symmetric stretch mode is Raman active but the asymmetric mode is not.

Infrared spectroscopy

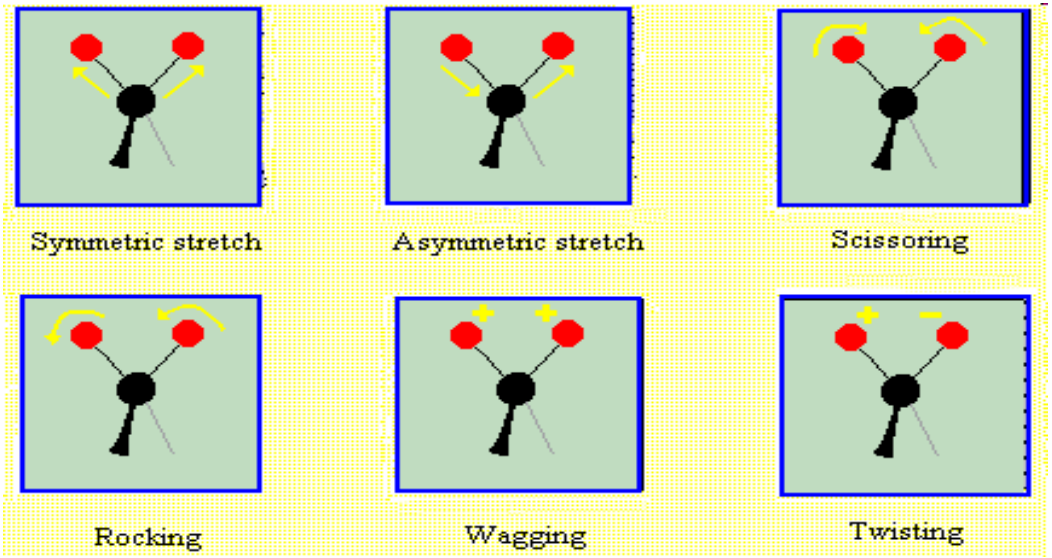

FTIR

Technique for collecting IR spectra is Fourier Transform Infrared (FTIR) spectroscopy. Instead of recording the amount of energy absorbed when the frequency of the IR radiation is varied by a monochromator, the IR radiation is guided through an interferometer. The purpose of the interferometer is to have a beam of IR radiation, split it into two beams, and make one of the beams travel a different (optical) distance than the other in order to create alternating interference fringes.

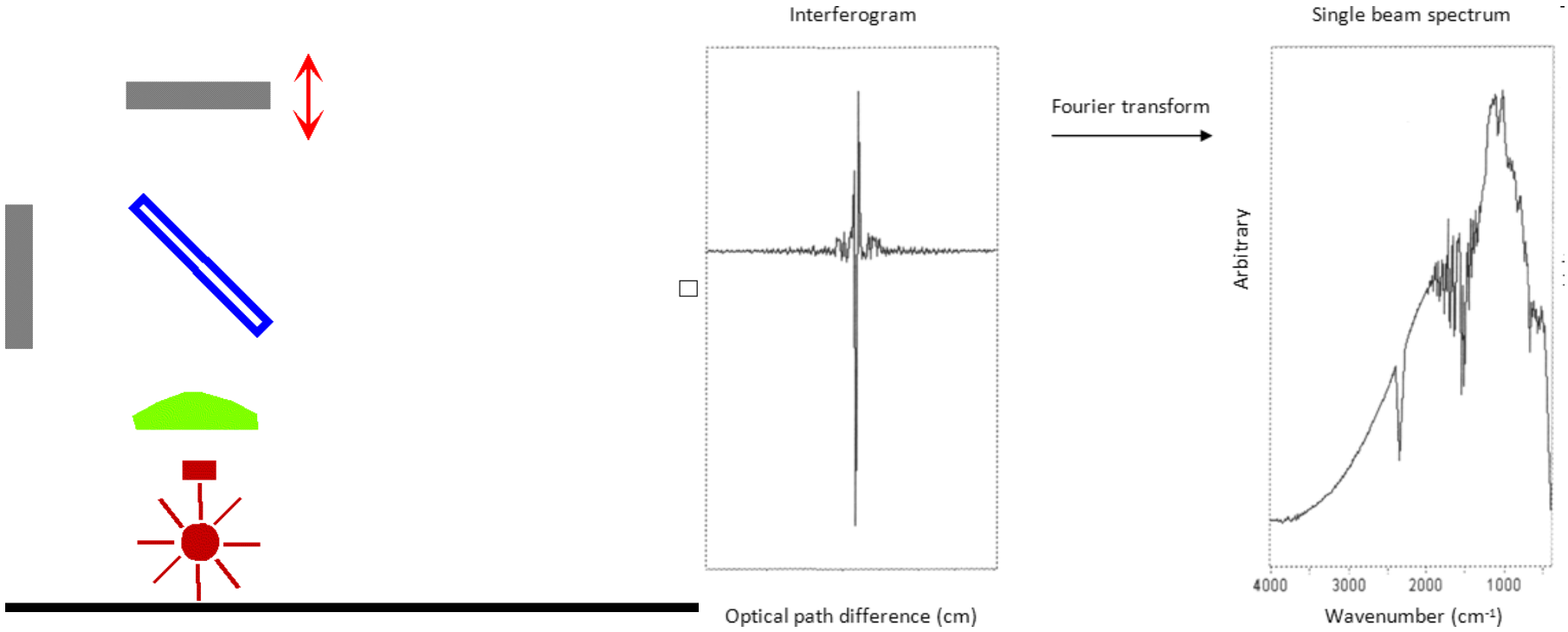

The beginning...

VO in Si

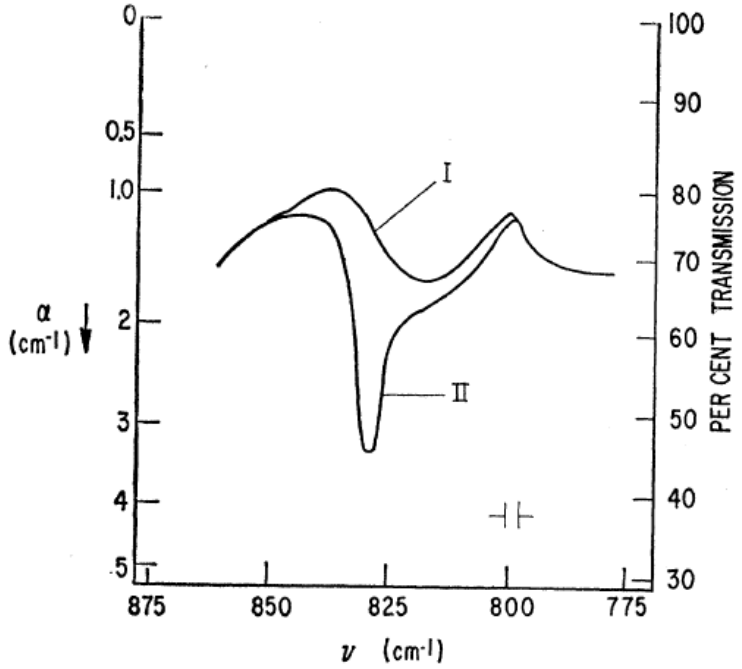

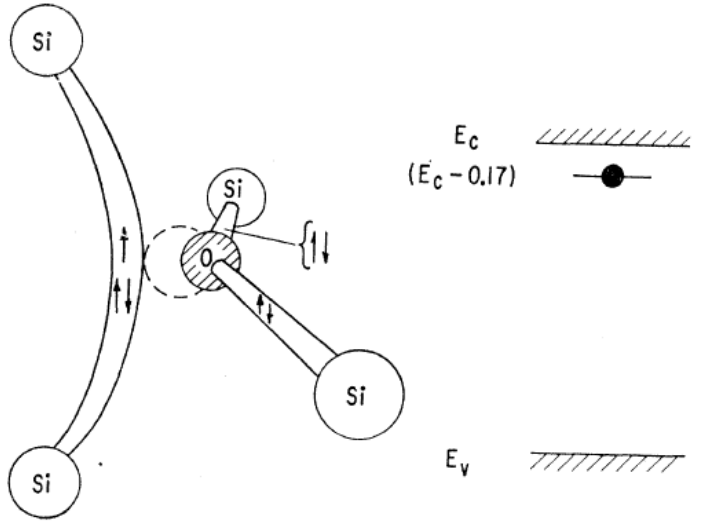

FIG. 11. Model of the *A* center showing the unpaired electron which gives rise to the spin resonance, in the Si-Si molecular bond. The associated electrical level is at $(E_c - 0.17$ ev).

[J. W. Corbett et al, Phys. Rev. 121, 1015–1022 (1961)]

VO (A-centre)

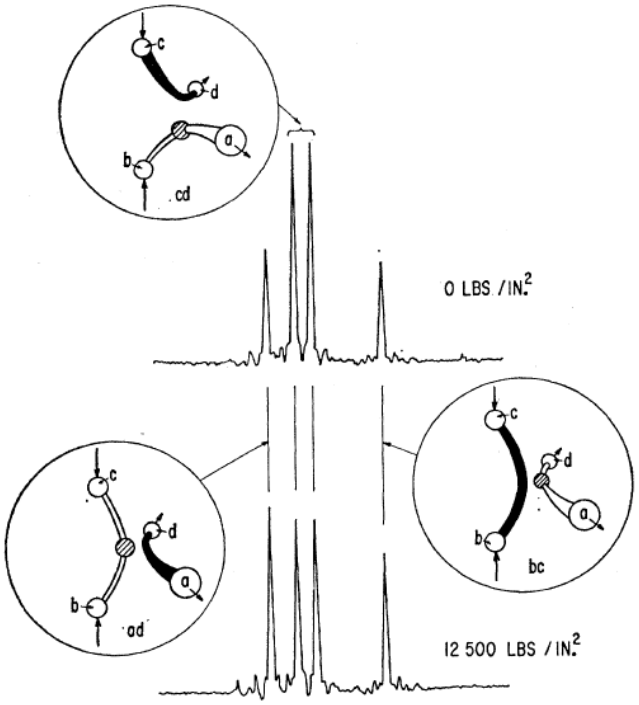

FIG. 12. Change in the spectrum resulting from *A* center reorientation under ⟨110⟩ stress. (The stress was applied at 125°K and the resulting alignment was frozen in by quenching to 77°K where the spectra were taken). The insets show the defect orientation corresponding to each multiplet.

EPR

[G.D. Watkins et al, Phys. Rev. 121, 1001–1014 (1961)]

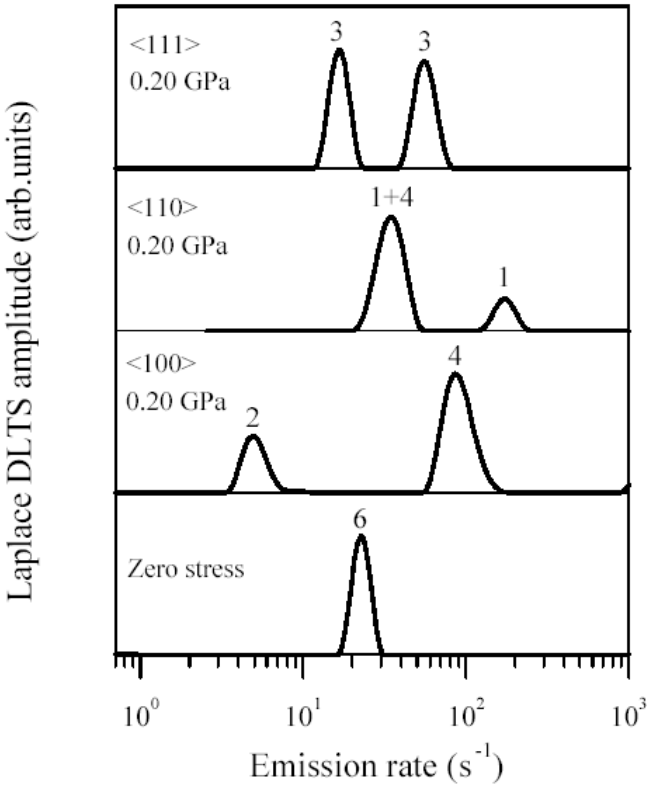

LDLTS

[L. Dobaczewski et al, Phys. Rev. B 67, 195204 (2003)]

Radiation Induced Defects and LVM

Infrared absorption studies of defect formation in Czochralski silicon irradiated with fast electrons in a wide range of temperatures (80–900 K) have been performed. The samples with different contents of oxygen and carbon were investigated. The main defect reactions are found to depend strongly on irradiation temperature and dose, as well as on impurity content and pre-history of the samples. Some new radiation-induced defects are revealed after irradiation at elevated temperatures as well as after a two-step (hot + room-temperature (RT)) irradiation.

$$V + O_i \rightarrow VO \quad (836\ cm^{-1}) \quad (1)$$

$$V + O_{2i} \rightarrow VO_2 \quad (895\ cm^{-1}) \quad (2)$$

$$VO + O_i \rightarrow VO_2 \quad (895\ cm^{-1}) \quad (3)$$

$$V + VO \rightarrow V_2O \quad (833\ cm^{-1}) \quad (4)$$

$$VV + O_i \rightarrow V_2O \quad (833\ cm^{-1}) \quad (5)$$

$$V + VO_2 \rightarrow V_2O_2 \quad (829\ cm^{-1}) \quad (6)$$

$$O_i + VO_2 \rightarrow VO_3 \quad (910, 976, 1005\ cm^{-1}) \quad (7)$$

$$I + O_i \rightarrow IO_i \quad (944, 956\ cm^{-1}) \quad (8)$$

$$I + IO_i \rightarrow I_2O_i \quad (936\ cm^{-1}) \quad (9)$$

$$I + O_{2i} \rightarrow IO_{2i} \quad (922, 1037\ cm^{-1}) \quad (10)$$

$$I + IO_{2i} \rightarrow I_2O_{2i} \quad (917, 1034\ cm^{-1}) \quad (11)$$

$$I + VO \rightarrow O_i \quad (1136\ cm^{-1}) \quad (12)$$

$$I + VO_2 \rightarrow O_{2i} \quad (1012, 1060\ cm^{-1}) \quad (13)$$

$$V + IO_{2i} \rightarrow O_{2i} \quad (1012, 1060\ cm^{-1}) \quad (14)$$

[J.L. Lindstrom et al. / Nucl. Instr. and Meth. in Phys. Res. B 186 (2002) 121–125]

e-irradiated Si
VO-related defects

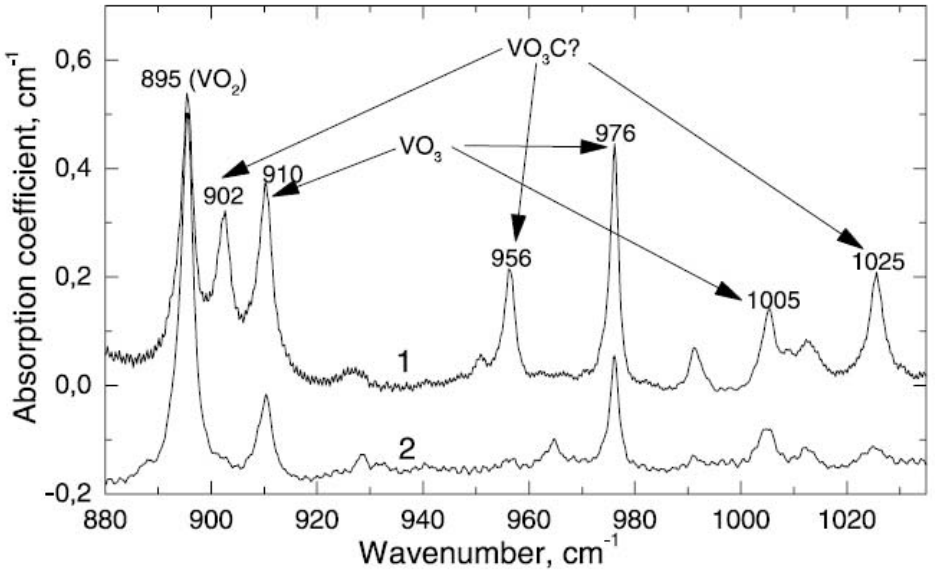

Fig. 1. Section of absorption spectrum measured at 10 K for carbon-rich CZ-Si ($[C_s] = 3 \times 10^{17}$ cm^{-3}) irradiated with electrons (1×10^{18} cm^{-2}) at (1) 770 K and (2) 300 K and then isochronally (30 min) annealed in 50 K steps up to 770 K.

[J.L. Lindstrom et al. / Nucl. Instr. and Meth. in Phys. Res. B 186 (2002) 121–125]

e-irradiated Si
VO-related defects

Infrared absorption from oxygen-related defects in Si crystals irradiated with electrons (2.5 MeV) at room temperature (RT) and in the range 300–600°C has been investigated. A band at 833.4 cm−1 is found to increase in strength upon annihilation of divacancies at 250–300°C. The **V_2O** complex is suggested to give rise to this band.

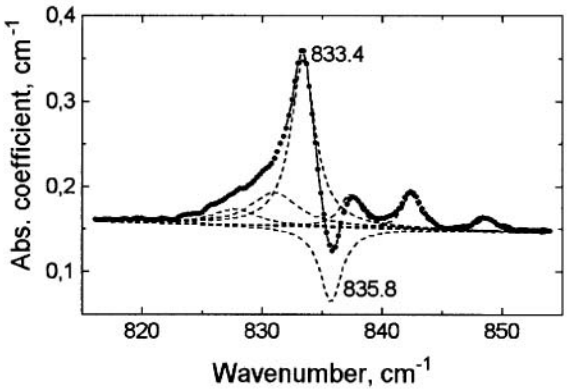

Fig. 4. Difference absorption spectrum at 10 K for sample 1 (see caption to Fig. 1) annealed at 300°C for 30 min. The spectrum recorded after irradiation was used as a reference. Dashed lines show a deconvolution of the spectrum onto the absorption peaks of Lorentzian shape.

[J.L. Lindstrom et al. / Physica B 273-274 (1999) 291-295]

V_2O as seen by DLTS

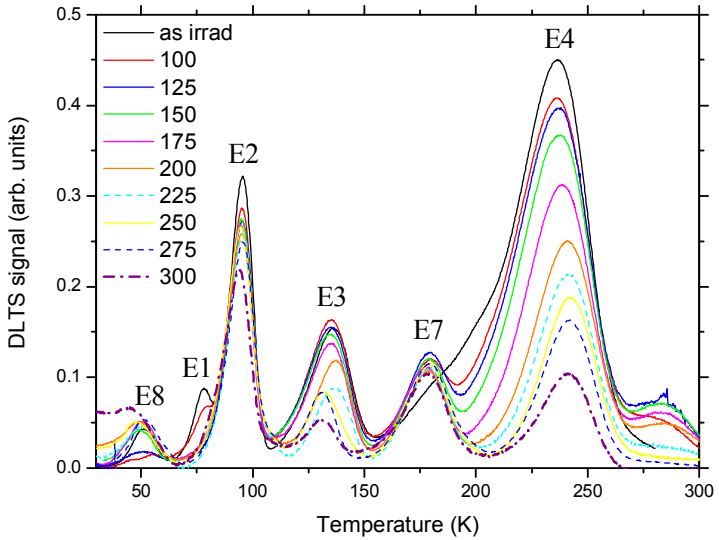

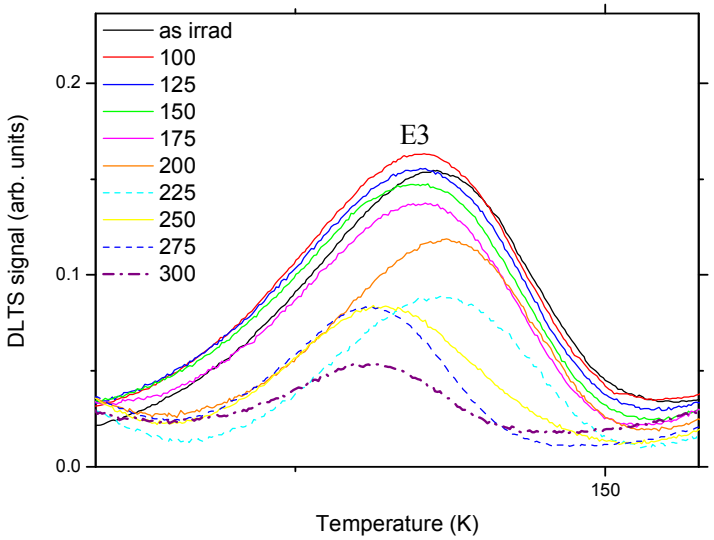

E3=> @ T >200 ºC → VV + O_i → V_2O

e-irradiated Ge

Infrared absorption at 10 K of oxygen-rich Ge crystals after irradiation with fast electrons (E=4 MeV, T≈100°C) and subsequent annealing at 220–420°C has been studied. It is found that upon heat-treatments of the irradiated samples at 220–280°C the simultaneous formation of four bistable thermal donors (TD1–TD4) occurs. This process is not accompanied by detectable changes in intensities of absorption bands at 780.4 and 818.0 cm−1, which are related to the oxygen dimer. Upon following anneals of the samples at 300–420°C, the strongly enhanced generation of the higher order TDs is observed with a simultaneous decrease in intensities of the bands originated from the oxygen dimer, TD1 and TD2. It is inferred that direct transformations of some radiation-induced defects into the first TD species occur in the irradiated samples. Radiation-induced complexes giving rise to local vibrational modes in the region 570–577 cm−1 and/or at 729, 733.5 and 745 cm−1 are suggested as possible precursors to the bistable TDs in Ge.

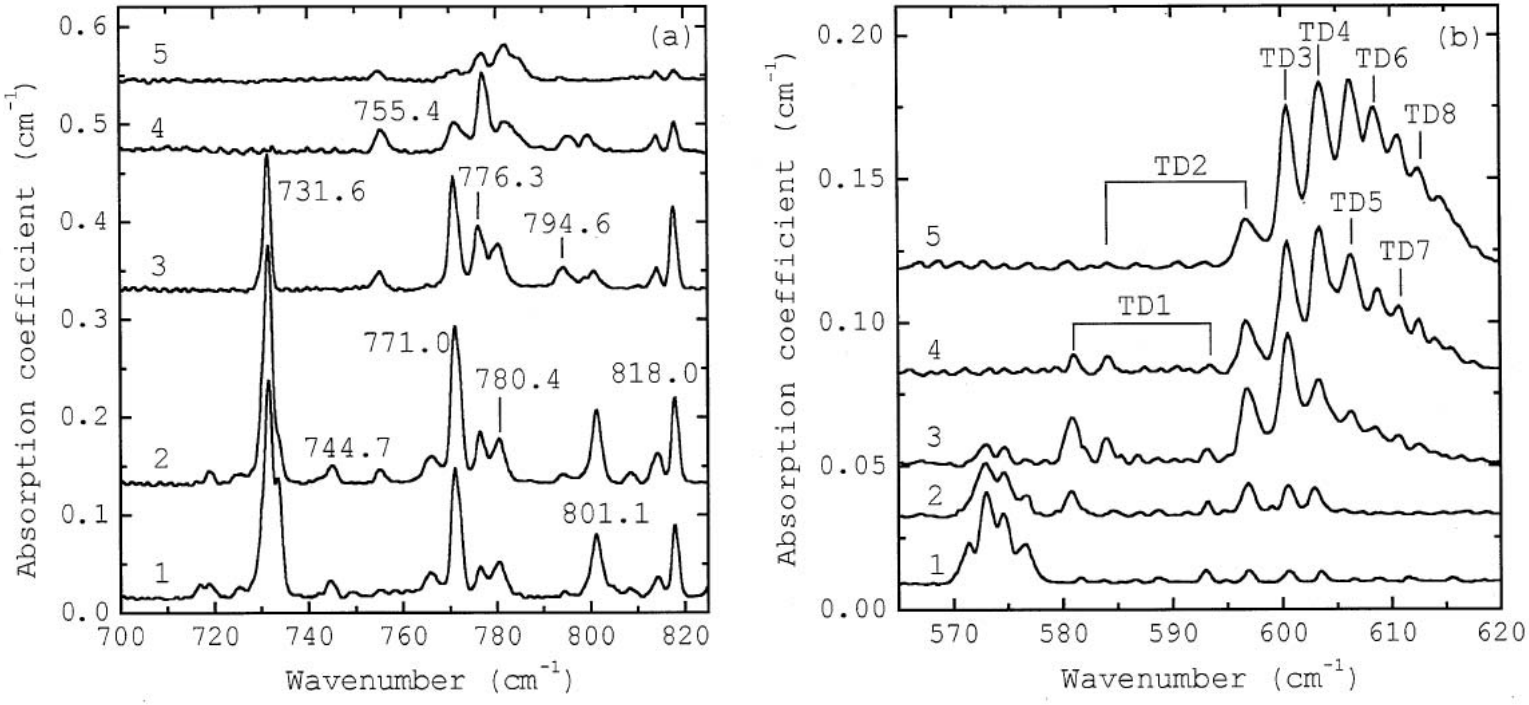

Fig. 1. Absorption spectra in the spectral regions of 700–825 cm^{-1} (a) and 560–620 cm^{-1} (b) at 10 K for Ge:Sb,O crystals after irradiation (1) and different stages of the subsequent isochronous (30 min) annealing at 240°C (2), 300°C (3), 360°C (4) and 420°C (5).

[B Langhanki et al, Physica B 302–303 (2001) 201–205]

24GeV proton irradiated Si

The irradiation doses and the concentrations of carbon and oxygen in the samples have been chosen to monitor the mobility of the damage products. Single vacancies and self-interstitials are introduced at the rate of 1 cm^{-1}, and divacancies at 0.5 cm^{-1}. Stable di-interstitials are formed when two self-interstitials are displaced in one damage event, and they are mobile at room temperature. In the initial stages of annealing the evolution of the point defects can be understood mainly in terms of trapping at the impurities. Damage clusters exist, and are largely removed by annealing at 700 to 800 K, when there is an associated loss of broad band emission between 850 and 1000 meV. The well-known *W* center is generated by restructuring within clusters, with a range of activation energies of about 1.3 to 1.6 eV, reflecting the disordered nature of the clusters. Comparison of the formation of the *X* centers in oxygenated and oxygen-lean samples suggests that the *J* defect may be interstitial related rather than vacancy related.

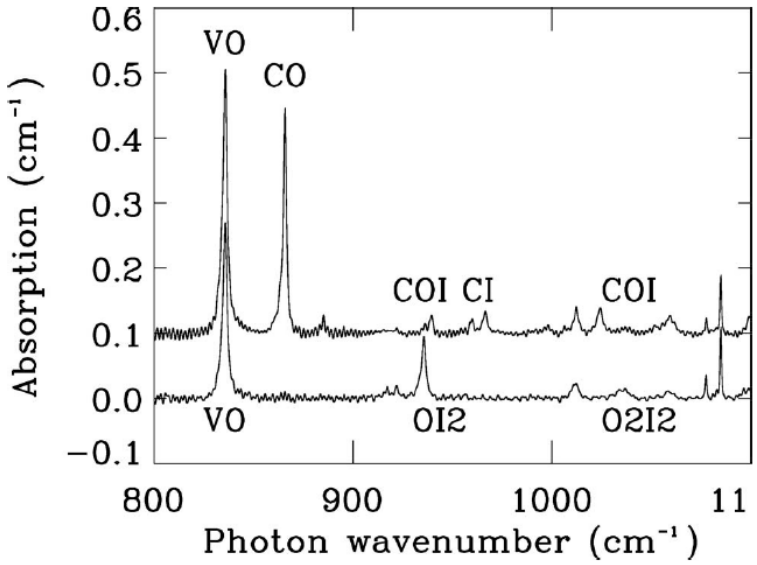

Infrared absorption measured at 20 K in oxygen-rich samples with high carbon upper curve, displaced by +0.1 cm^{-1} for clarity and low carbon lower curve. Radiation-induced peaks are labeled by their chemical origin, where for clarity the oxygen and carbon interstitials are simply labelled O and C. *I* is a selfinterstitial, O2 the oxygen dimer, and 2*I* two self-interstitials. The 'CI' peak is a doublet. Other peaks are caused by oxygen interstitials and oxygen dimers

[G. Davies et al, Phys Rev B **73**, 165202 2006]

IR & modelling

Infrared absorption experiments and *ab initio* computer simulations are used to study tin-carbon centers in silicon. Electron irradiation of C and Sn doped Si leads to prominent absorption lines at 873.5 and 1025 cm[1]. These are assigned to a carbon interstitial trapped by a substitutional Sn atom. The calculated modes are in good agreement with those observed. The calculations also suggest that a close-by pair of substitutional C and Sn will be a stable but electrically inert defect. This defect may account for the experimentally observed drop in the concentration of the C*s*-C*i* defect after a room temperature annealing. Finally, we suggest Sn-C codoping of Si for manufacturing of radiation hard silicon.

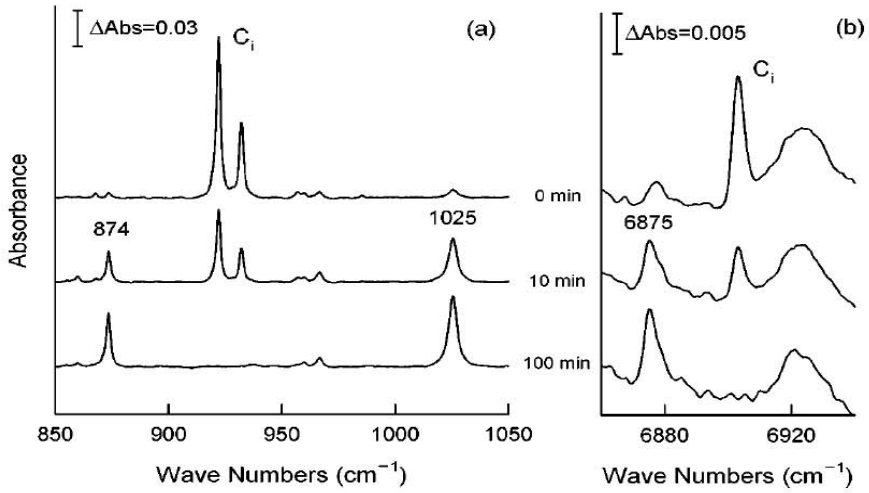

FIG. 1. Sections of absorbance spectra of electron irradiated (5×10^{17} cm^{-2}) Si:C:Sn recorded at 10 K: just after electron irradiation at 200 K, after 10 and 100 mins of room temperature annealings.

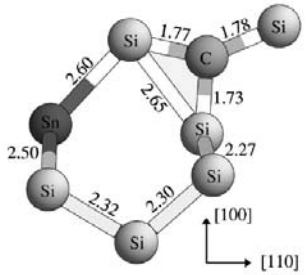

FIG. 3. Ground state configuration of the C_i-Sn_s center. The tin atom is at the next nearest neighbor position from both atoms of the C_i. Bond lengths are in [Å].

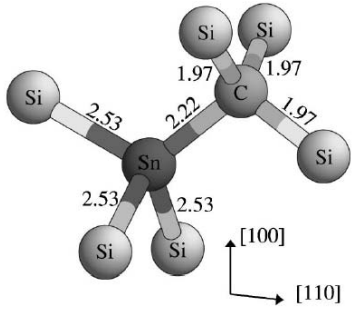

FIG. 4. The lowest energy structure for the C_s-Sn_s center in which a tin atom is located next to carbon. Both atoms are near the substitutional sites. Bond lengths are in [Å].

[E. V. Lavrov et al, Phys Rev B **64** 125212]

VO, VOH, VOH_2...

Hydrogen in Si!!!

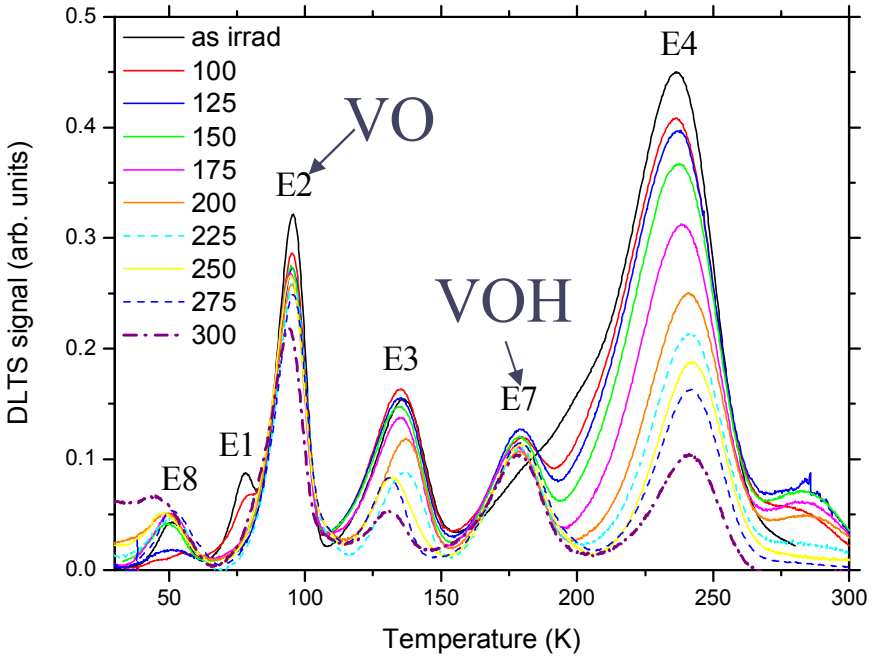

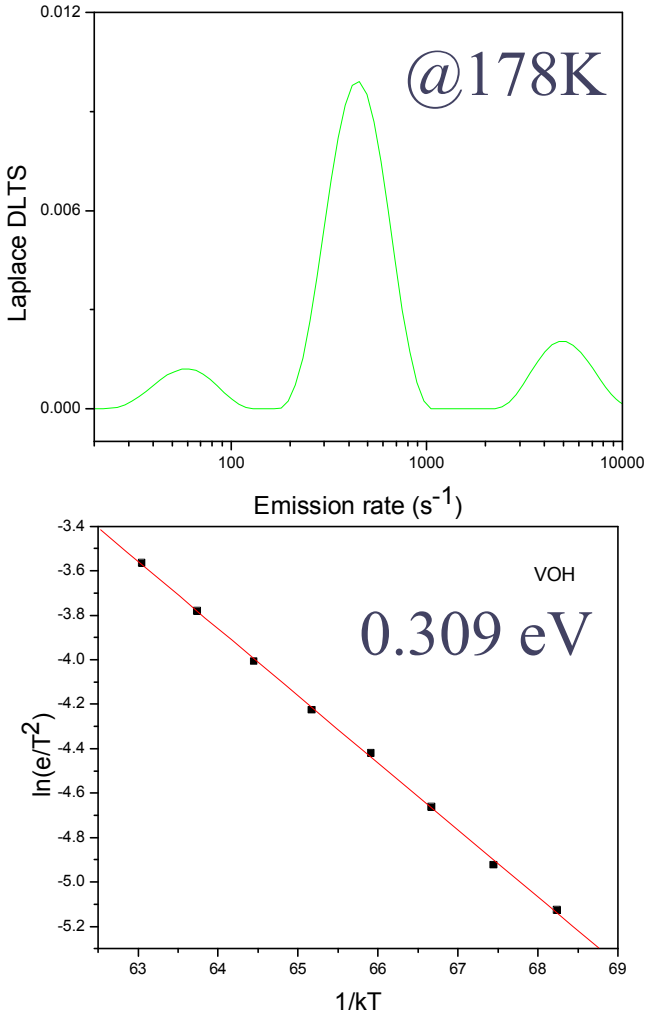

IR & modelling

VOH_2

The interaction of hydrogen with radiation-induced defects ~RD's! in Czochralski-grown silicon crystals has been studied by infrared-absorption spectroscopy and *ab initio* modeling. Hydrogen and/or deuterium was introduced into the crystals by indiffusion from H2 (D2) gas at 1200–1300 °C. The samples were subsequently irradiated with fast electrons and annealed in the temperature range of 100–600 °C. The centers produced by the irradiation were the same in both the untreated and treated cases, namely the *A*-center, C*i*-O*i* complex, and divacancy. A heat treatment of the H-treated samples resulted in the enhanced loss of these centers and the formation of centers containing hydrogen. The disappearance of the *A* centers in the temperature range of 100–150 °C is correlated with the appearance of three local vibrational modes LVM's at 943.5, 2126.4, and 2151.5 cm^{-1}.

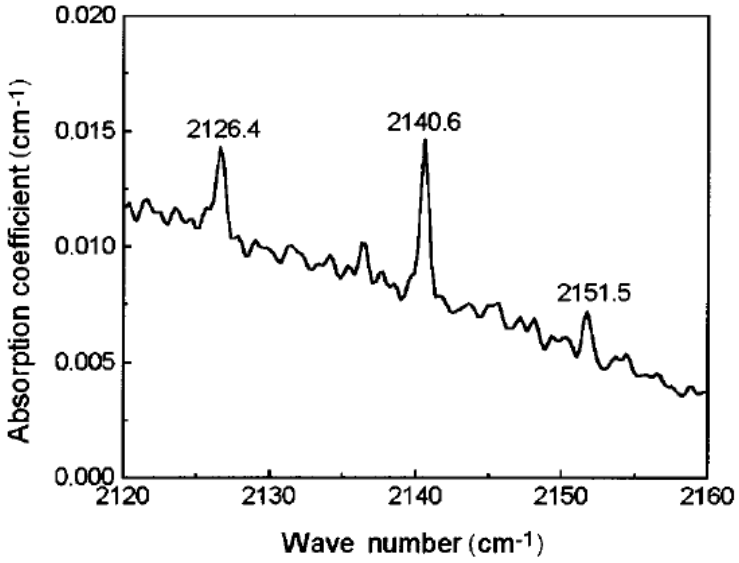

FIG. 6. Infrared-absorption spectrum, measured at 10 K, for a Cz-Si sample which was co-doped with hydrogen and deuterium, irradiated with fast electrons, and annealed at 100 °C for 105 h.

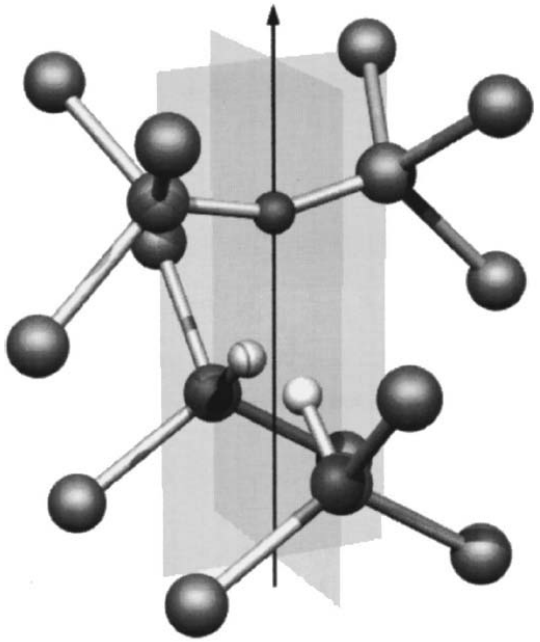

FIG. 7. Calculated ground-state structure for the *V*-O-H_2 center in silicon. Oxygen is over the C_2 axis, and the white atoms represent hydrogen.

[V. P. Markevich et al, Phys. Rev. B 61, 12964 (2000)]

Photoluminescence

- Excite the sample with light (‘photo’); some of the energy is emitted as light (‘luminescence’).
- Photoluminescence (abbreviated as PL) is a process in which a substance absorbs photons (electromagnetic radiation) and then re-radiates photons. Quantum mechanically, this can be described as an excitation to a higher energy state and then a return to a lower energy state accompanied by the emission of a photon.
- Excitation is usually by a laser, for convenience of directed beam, with beam power of 100’s of mW.
- Electron-hole pairs (excitons) are created with a lifetime of 10’s of ms in pure Si. They are captured by traps (impurities).
- Photon emitted by exciton decay has energy characteristic of the trap.

Introduction to PL

What can we observe?

Only (usually) neutral centres.

Very sharp optical transitions: energy resolution typically 0.1 meV at 1000 meV.

Each sharp line is characteristic of one atomic-sized defect.

The PL spectrum at low sample temperatures often reveals spectral peaks associated with impurities contained within the host material. The high sensitivity of this technique provides the potential to identify extremely low concentrations of intentional and unintentional impurities that can strongly affect material quality and device performance. Concentrations over 10^{11} cm^{-3}. Best 10^{14} to 10^{16} cm^{-3}.

Require:

Samples with transparent surfaces (no contacts).

Samples of about 8 x 8 mm2.

(It is a non-destructive technique!)

Samples at T < 20 K.

Photoluminescence

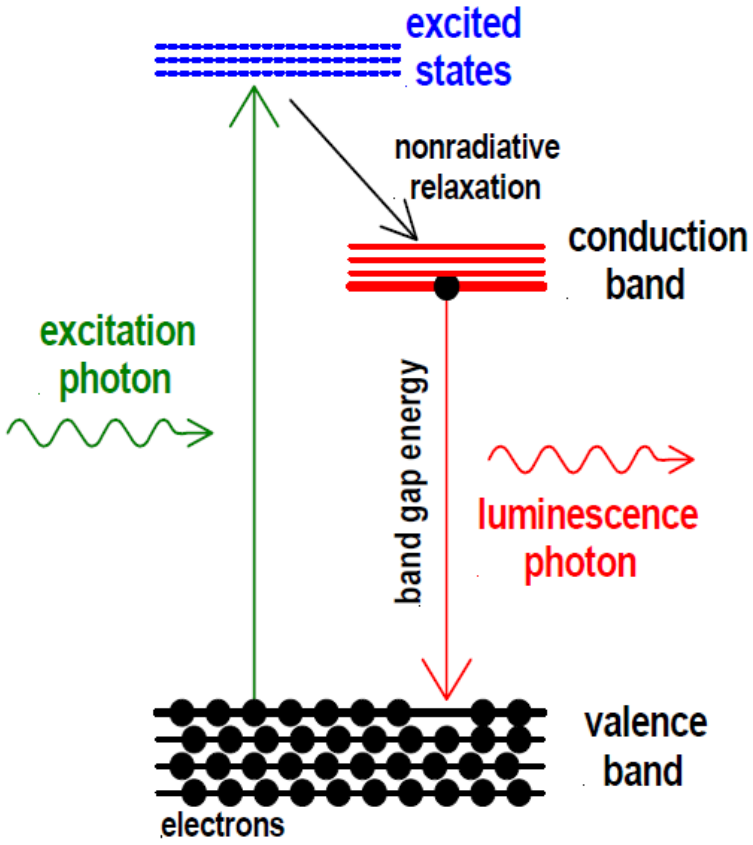

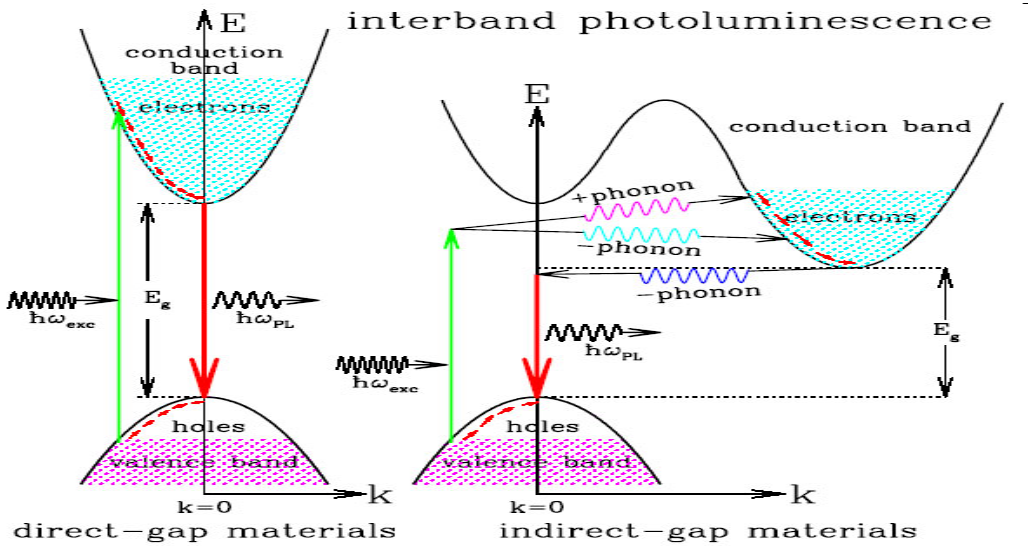

Photoluminescence

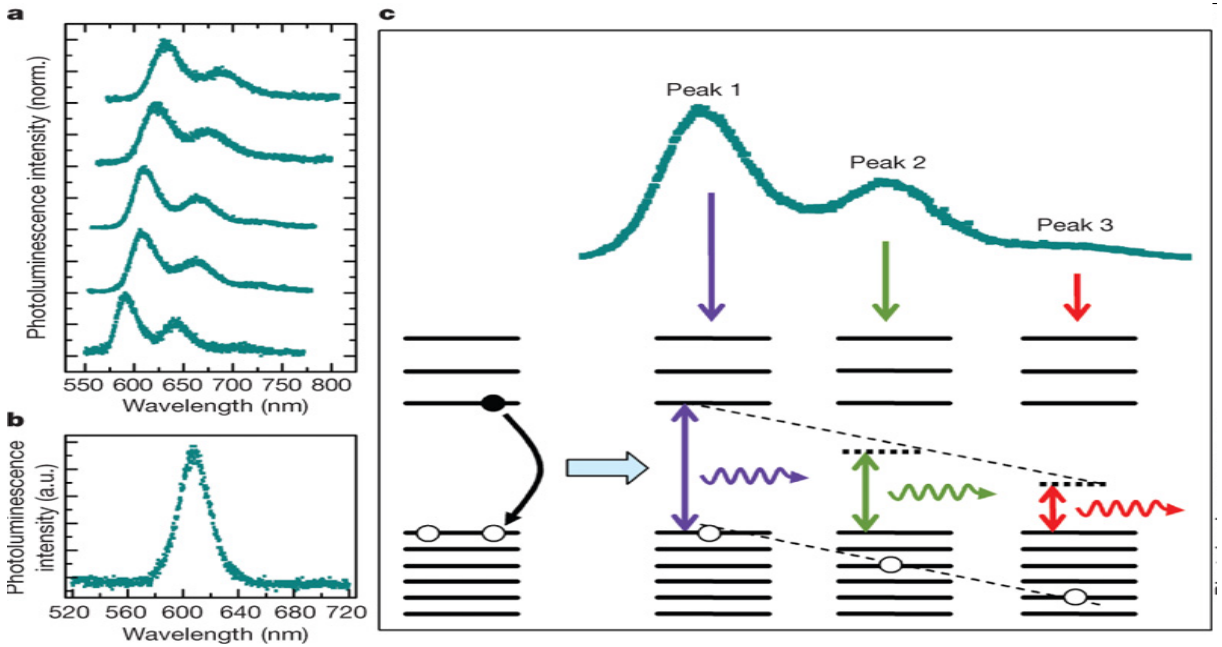

Xiaoyong Wang, Xiaofan Ren, Keith Kahen, Megan A. Hahn, Manju Rajeswaran, Sara Maccagnano-Zacher, John Silcox, George E. Cragg, Alexander L. Efros & Todd D. Krauss

Nature 459, 686-689(4 June 2009)

Photoluminescence

Case study: small Si-interstitial clusters in Si

Rodlike {311} defects are commonly observed in ion-implanted silicon and are believed to play important roles in boron transient enhanced diffusion (TED) by providing interstitials during annealing processes. While the structural properties of rodlike {311} defects are well characterized by experiments, e.g., via high resolution transmission electron microscopy (HRTEM) the existence and properties of small clusters are not well understood.

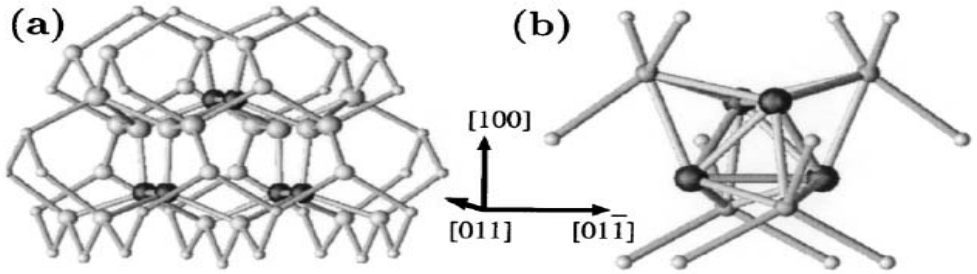

FIG. 2. Atomic structures of tri-interstitial clusters: (a) elongated configuration of C_{1h} symmetry and (b) compact configuration of D_{2d} symmetry. Both clusters contain dumbbell interstitials shown as solid black atoms as the building blocks. The elongated tri-interstitial cluster (a) contains three [011]-oriented dumbbells side by side in the [01$\bar{1}$] direction. On the other hand, the compact tri-interstitial cluster (b) has two dumbbells having different orientations parallel to the [011] and [01$\bar{1}$] directions.

[J. Kim et al, Physical Review Letters 84 (2000) 503-506]

Why clusters?

This SRIM simulation of a 1MeV As ion in Ge shows high concentration clusters of primary defects which react to form stable complexes eg V2 , V3 or larger clusters of vacancies or interstitials eg extrinsic stacking faults.

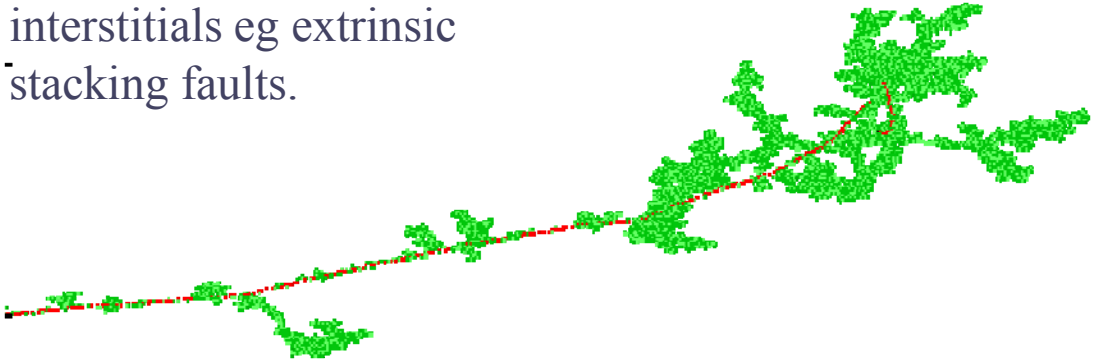

Vacancy cluster in Si

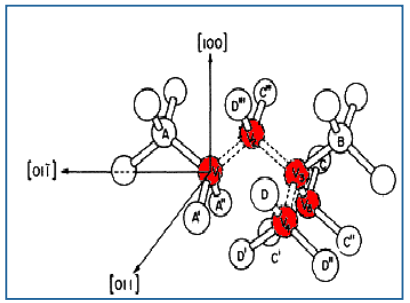

$Si^{+} \rightarrow nSi$

- Samples of *n*-type (100) Cz silicon of resistivity 6–8 Ωcm ($5–8 \times 10^{14}$ phosphorus cm^{-3}) were implanted with 5.6 MeV $^{28}Si^{3+}$ ions at room temperature with doses of 10^{9} - 10^{14} cm^{-2} using the 1.7 MV NEC Tandem accelerator. The implanted samples were annealed for 30 min at 525 or 750 °C in a tubular oven under constant argon flow.

[D.C.Schmidt et al, J. Appl. Phys. 88, 2309 (2000)]

$Si^+ \rightarrow nSi$

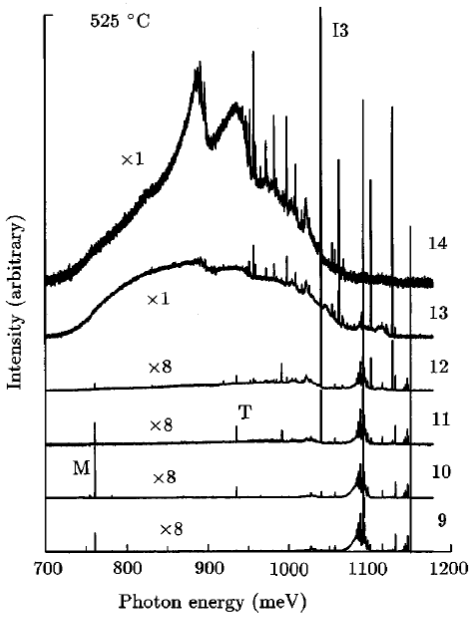

FIG. 1. An overview of the PL spectra at 4.2 K from samples implanted with doses from 10^9 cm^{-2} (labeled "9," bottom spectrum) to 10^{14} cm^{-2} (labeled "14," top spectrum) and annealed for 30 min at 525 °C. The strengths of representative sharp-line features are given in Fig. 3. PL at energies greater than 1030 meV in the 10^9 cm^{-2} spectrum (and replicated in the others) is produced by phosphorus, boron, free excitons and the electron-hole plasma and is not of fundamental interest here. For clarity the spectra are displaced vertically; the zero level is shown by the high energy end of each spectrum.

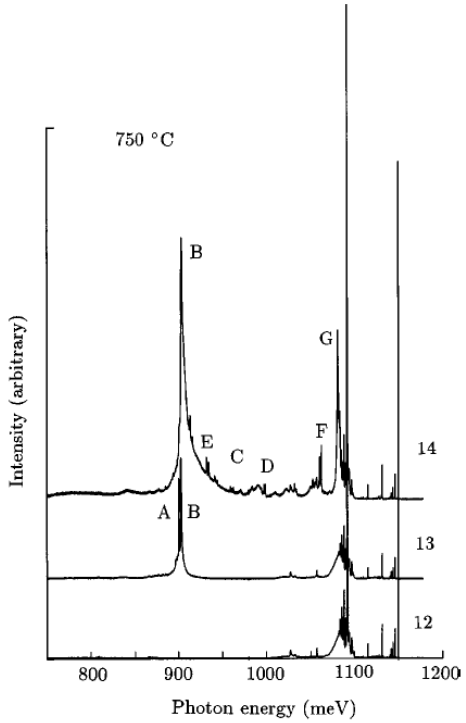

FIG. 6. PL spectra at 4.2 K of samples implanted with 10^{12}–10^{14} cm^{-2} (labeled "12"–"14") and annealed at 750 °C. Samples implanted below 10^{12} cm^{-2} gave spectra indistinguishable from the 10^{12} cm^{-2} implant. The features labeled A through G are discussed in the text. PL at energies greater than 1030 meV in the 10^{12} cm^{-2} spectrum (and replicated in the others) is produced by phosphorus, boron, free excitons and the electron-hole plasma. For clarity the spectra are displaced vertically; the zero level is shown by the ends of each spectrum.

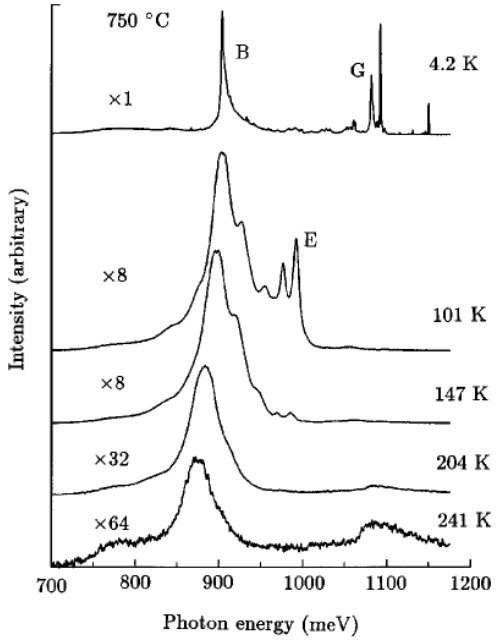

FIG. 7. PL spectra at 4.2–240 K of samples implanted with 10^{14} cm^{-2} and annealed at 750 °C. The intensities have been multiplied by the factors shown for each displayed spectrum. Features "*B*," "*E*," and "*G*" are in Fig. 6. Note that with increasing temperature the luminescence towards higher energy is lost first, as the shallower excited states are thermally ionized; the band starting near 1060 meV at 240 K is free-exciton emission. For clarity the spectra are displaced vertically; the zero level is shown by the left end of each spectrum.

[D.C.Schmidt et al, J. Appl. Phys. 88, 2309 (2000)]

$Si^+ \rightarrow nSi$

As seen by DLTS

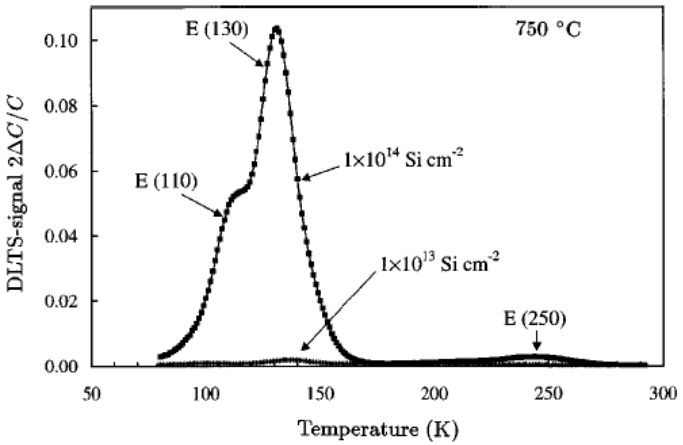

FIG. 4. DLTS spectra of the samples implanted with doses of 10^{13} and 10^{14} cm^{-2} following a 30 min anneal at 750 °C. The reverse bias was −10 V; the filling pulse was 10 V; and the rate window was $(640\ ms)^{-1}$. For lower doses no defect levels were detected in the DLTS spectra. The defect level $E(250)$ is strongest in the 10^{14} cm^{-2} spectrum.

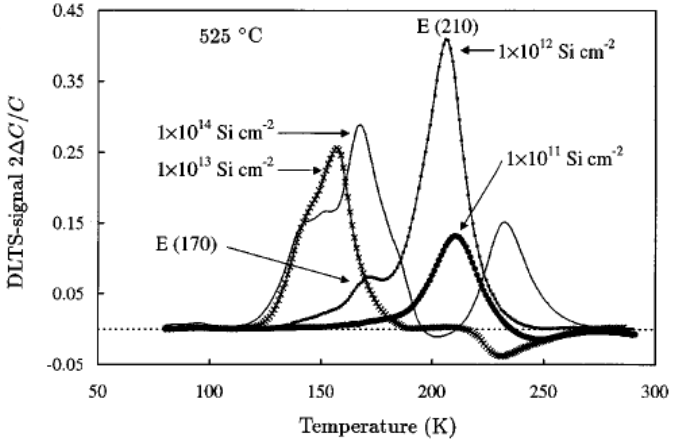

FIG. 10. DLTS spectra of the samples implanted with doses from 10^{11} to 10^{14} cm^{-2} and annealed for 30 min at 525 °C. The reverse bias was −10 V; the filling pulse was 10 V; and the rate window was $(640\ ms)^{-1}$. For doses greater than 10^{12} cm^{-2} the defect concentrations are too high for accurate DLTS measurements with the shallow dopant levels ($\sim 6\times10^{14}$ cm^{-3}) used here.

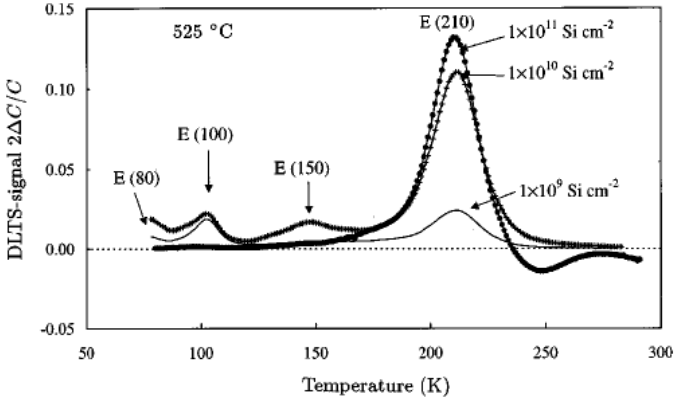

FIG. 9. DLTS spectra of samples implanted with doses from 10^{9} to 10^{11} cm^{-2} following a 30 min anneal at 525 °C. The reverse bias was −10 V; the filling pulse was 10 V; and the rate window $(640\ ms)^{-1}$.

[D.C.Schmidt et al, J. Appl. Phys. 88, 2309 (2000)]

$Si^+ \rightarrow nSi$

- For samples annealed at 750 °C, line broadening is only significant at the highest doses for two transitions: the 1080 meV PL and for the 903 PL produced by the self-interstitial aggregates of the {113} defect
- In samples annealed at 525 C ... Interstitial clusters

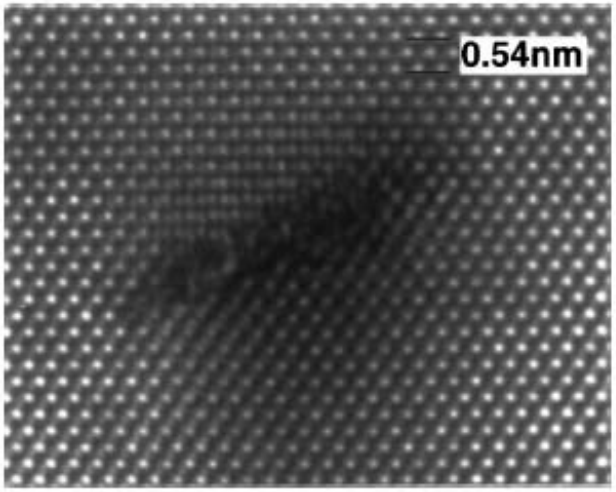

FIG. 8. Transmission electron lattice image of a {113} defect with a width of 5 nm in a sample implanted with 10^{14} cm^{-2} Si ions and annealed at 750 °C.

[D.C.Schmidt et al, J. Appl. Phys. 88, 2309 (2000)]

Neutron irradiated Si

- n- irradiated FZ-Si and MCz-Si (MCz <100>, 1kΩcm, 300 μm and 2-3mm thick ([Oi] = 5x1017 cm-3, [Cs] < 5x1015 cm-3, FZ 288μm and 3mm thick , 2kΩcm)
- tri-interstitials silicon – line W (I3) (1.018eV)
- tetra-interstitials silicon – line 1.039eV (I4)

[Barbara Surma, Paweł Kamiński, Artur Wnuk and Roman Kozłowski, Nuclear Science Symposium Conference Record, 2008. NSS '08. IEEE]

PL emission at 18K for n-irradiated FZ-Si and MCz-Si (fluence $3x10^{15}$ n/cm^2) vs. annealing temperature for isochronal annealing

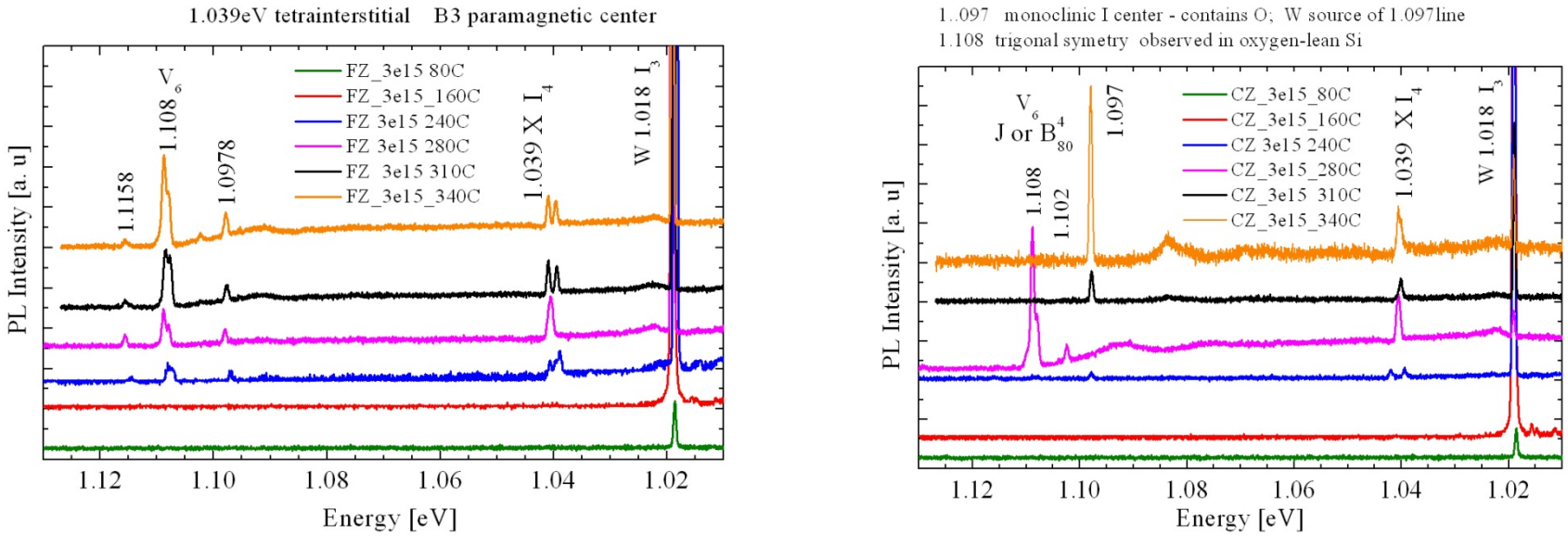

[Barbara Surma, Paweł Kamiński, Artur Wnuk and Roman Kozłowski, Nuclear Science Symposium Conference Record, 2008. NSS '08. IEEE]

Are tri-interstisials (W) the precoursors for the formation of tetra-interstitials (I4)?

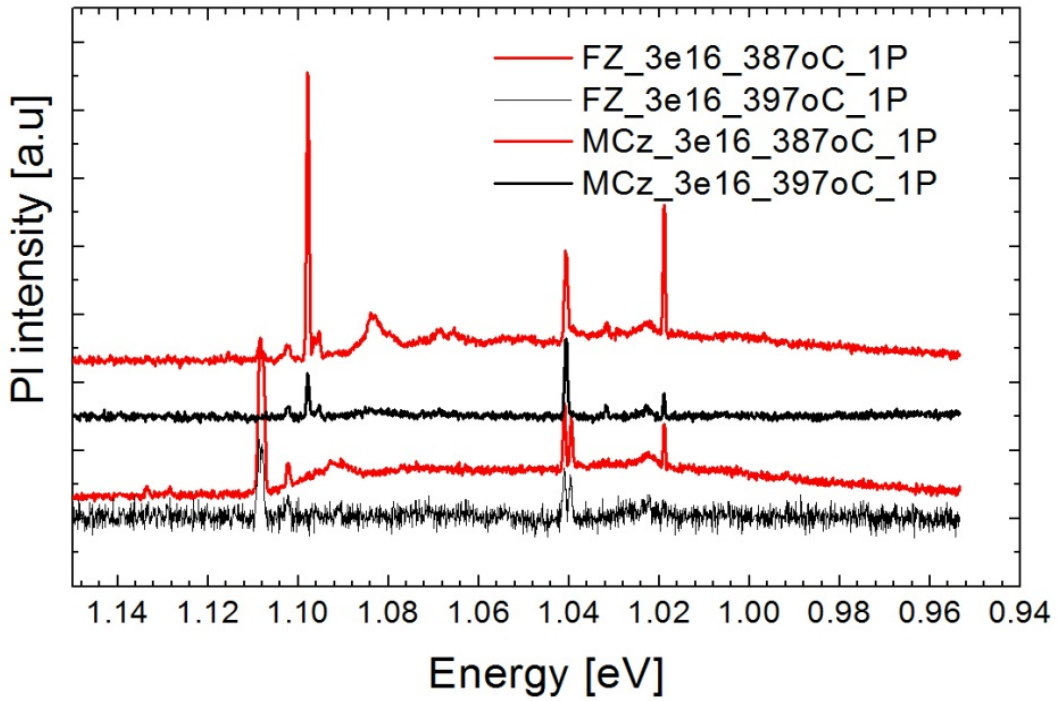

[Barbara Surma, Paweł Kamiński, Artur Wnuk and Roman Kozłowski, Nuclear Science Symposium Conference Record, 2008. NSS '08. IEEE]

24GeV proton irradiated Si

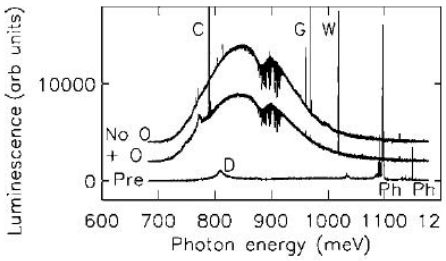

FIG. 4. Preirradiation, both materials show identical luminescence above 1000 meV from the phosphorus donors ("Ph") plus weak free-exciton emission. The oxygenated material, labeled "Pre," also contains weak dislocation bands at 808 and 874 meV. After irradiation, the high-energy luminescence is quenched, and both materials show a broadband between about 750 and 1000 meV, plus weak *W* emission at 1018 meV. In the oxygenated sample ("+O"), carbon interstitials have been trapped preferentially at oxygen, forming the C center (789 meV), and in the nonoxygenated sample ("No O") preferentially at substitutional carbon, creating the *G* center (969 meV). The sharp absorption lines and the dip near 800 meV are from atmospheric and instrumental absorption. The spectra shown here were measured at 4.2 K and at 60 μeV resolution.

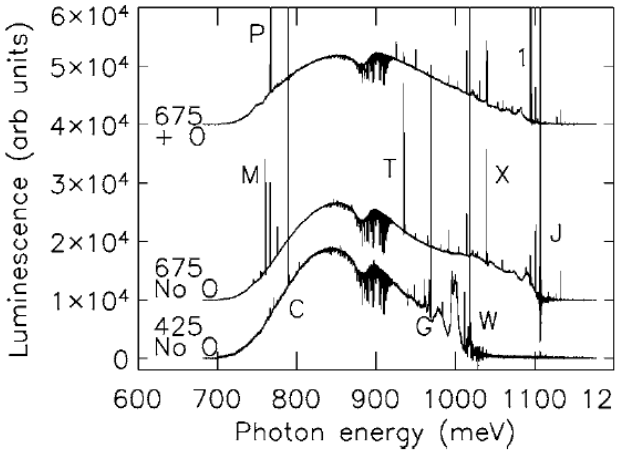

FIG. 7. After 425 K annealing, both materials are developing strong, and identical, *W* bands. The nonoxygenated sample shown here, bottom spectrum, has the *G* (969 meV) and *C* (789 meV) lines; the oxygenated has a negligible *G* line and the *C* line is 4.5 times stronger. By 675 K, the strongest features are the *J* lines in the nonoxygenated (second spectrum from bottom), and the 1096 meV line, labeled 1, and the *P* line in the oxygenated material (top spectrum). The sharp absorption lines and the dip near 800 meV are from atmospheric and instrumental absorption. The spectra shown here were measured at 4.2 K and at 60 μeV resolution.

C line → C_iO_i; G line → C_iC_s ; T line → C_2H; W line → small interstitial clusters;

X line → tetrainterstitial?

[G. Davies et al, Phys Rev B **73**, 165202 2006]

Clusters as seen by LDLTS

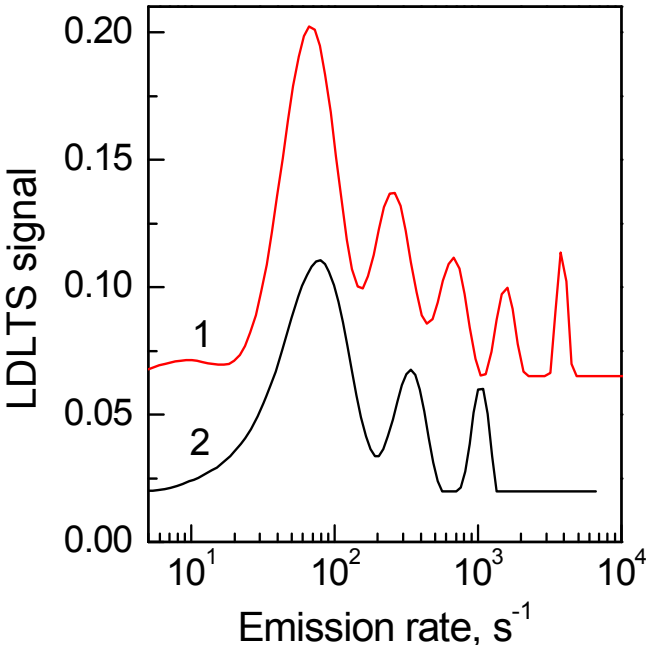

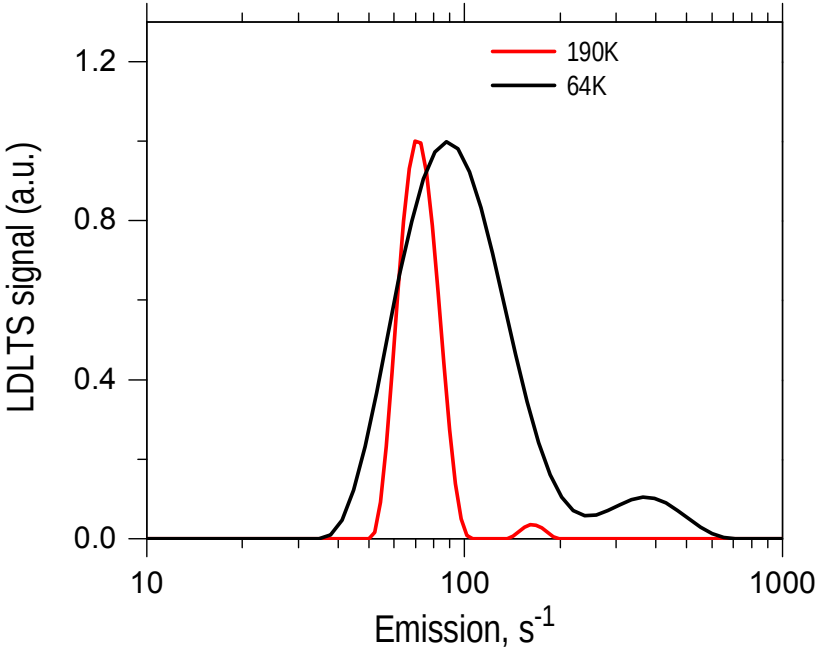

[I. Kovacevic et al,J. Phys.: Condens. Matter 17 (2005) S2229]

[A.R. Peaker et al, Solid State Phenomena 131-133 (2008) 125]

Conclusions

- Radiation introduces electrically active and non-active defects.
- One ring to rule them ALL?